Detector

FOPRA No. 77

Date Performed: 18 and 25 May, 2018
TU Muenchen, Garching

Authors: Bryan Chambers (b.chambers@tum.de)
Caroline Dahlqvist (caroline.dahlqvist@tum.de)

Supervisor: Phillipp Klenze (pklenze@ph.tum.de)

Theory & Background

We will investigate nuclear decay process by doing a real life experiment and using a simulation. The purpose is to determine the accuracy and validity of a simulation. Simulations can save precious money and time, for example if we can do a simulation before building an actual detector we can know valuable answers to key questions such as; 'Where is the best place to put my detector(s)? What geometry or design best serves the experiment?' But we should first know that the simulation is indeed reliable and produce accurate results by comparing it to a real experiment and that is what we did. We will discuss the results and observations we accrued.

The type of detector we used is a Cesiumiodine (CsI) scintillating crystal coupled with Avalanche Photodiode (APD). The source of radiation is 22-Na that will provide γ-rays. There are two different unique processes that will produce radiation that will be detected. In the first one our sodium source decays into Neon atom in its excited state through a beta decay process and that will result in a positron and electron neutrino after which the positron collides with an electron in the plastic material surrounding the source and that produces two 0.511 MeV gamma photons (electron-positron annihilation).

$$Na_{22} \rightarrow Ne^{*}_{22} + e^{+} + \nu_e$$
$$e^{+} + e^{-} \rightarrow 2\gamma \ \ (0.511 \text{ MeV})$$

The other decay process of interest in simply the de-excitation of the Neon atom, and this creates our 1.275 MeV gamma rays.

$$Ne^{*} \rightarrow Ne + \gamma \, (0.511 \text{ MeV})$$

There are other quantum mechanical processes that occur in the scintillator. Namely the photoelectric effect, Compton scattering, and pair production due to the electrons produced by the photoelectric effect. How much of this radiation is produced depends on the type of scintillator used. We will detect a full spectrum of radiation due to these quantum mechanical process but we will not investigate it. We will analyze only the peaks of the 0.511 MeV and the 1.275 MeV gamma rays. Using the right type of scintillator is not trivial as they each have different densities and therefore different stopping powers of the scattered electrons, and produce various values of scattered radiation based on the amount of radiation absorbed. Changing the scintillator can result in better or worse resolution for the peaks we analyze.

Inside of the detector the inner surface of it is covered with a reflective material to increase the efficiency of detected photons. It should be mentioned that the detector does not actually detect individual particles that we are interested in directly, in this case the the 0.511 and

1.275 MeV gamma rays. What actually happens is the gamma rays create a cascade of particles called an *electromagnetic shower,* the number of these secondary photons produced is proportional to the energy of the incident gamma rays.

These produced photons, after passing through the scintillating material are detected by an (APD), an avalanche photodiode. The ADP is a silicon doped semiconductor which creates a current proportional to the photon flux. The histograms of the counts versus energy and Gaussian fits were generated by ROOT. The simulations and data readout of the experiment were done with GEANT.

The experimental setup consists of a source and detectors placed on either side of it, placed approximately 4.96 cm away, illustrated in fig.1. When running the simulations the dimensions of all parameters in the experiment are replicated, such as distance of detectors from the source, material of scintillator, geometry of source with isotropic radiation aand housing dimensions all in order to achieve the highest accuracy possible.

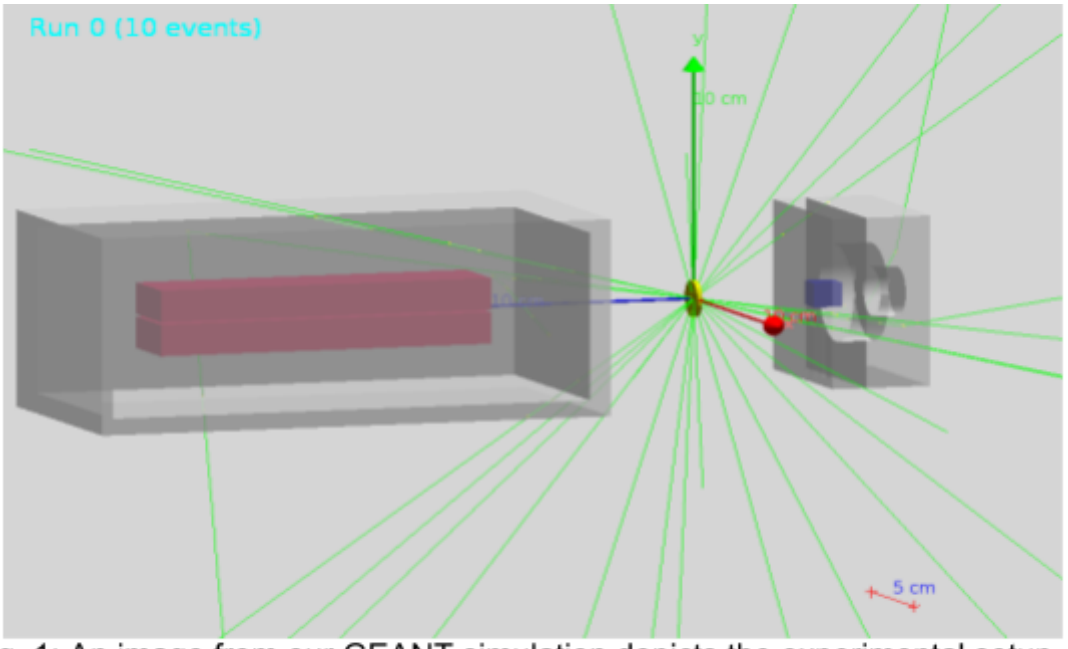

Fig. 1: An image from our GEANT simulation depicts the experimental setup. To the left we have our large detector with two crystals in the center separated by 1.0mm with dimensions of (29mm)x(13mm)x(130mm) and Al housing of (100mm)x(81mm)x(200mm). To the right we have our small detector with dimensions of (30mm)x(35mm)x(19mm) with two cylinders cut out of radii of 10mm and 5.0mm and a hole in the bottom of radius 3.5 mm and thickness of 14mm. The source for gamma rays located in the middle of the two detectors at a distance of 4.95.

Detector Efficiency

As the detector(s) do not encompass the entire region of space through which the radiation permeates (in both the simulation and actual experiment) and not all radiation that enters the detector(s) is actually measured, therefore there is an efficiency factor which we are concerned with. The geometric efficiency can be understood as the fraction of surface area of a sphere the detector covers divided by the solid angle of a sphere. The solid angle of the detector whose incident surface is a rectangle is given by:

$$\Omega = 4 \arctan \frac{\alpha\beta}{2d\sqrt{4d^2 + \alpha^2 + \beta^2}}$$

Where α and β are the lengths of the face of the detector, and d is the distance of the detector from the sodium source. The geometric efficiency therefore is

$$\varepsilon_{geo} = \frac{\Omega}{4\pi}$$

The total efficiency, empirically is just the fraction of the number of gamma rays detected to the emitted of that particular energy peak, it can also be equated as the product of the geometric and performance efficiency of the detector itself.

$$\varepsilon_{tot} = \frac{N_{detected}(E)}{N_{emitted}(E)} = \varepsilon_{geo} \cdot \varepsilon_{det}$$

We will be calculating ε_{det} for both simulation and experiment and comparing them in our analysis.

Detector Resolution

The resolution is defined as the distinguishability between two peaks. The formula used for calculating the relative resolution is

$$R = \frac{FWHM}{\mu} = \frac{\sigma * 2 * \sqrt{2 * ln(2)}}{\mu}$$

Where μ is the mean value of the the (Gauss) fitted peak and σ is the standard deviation of it. In this experiment the resolution of a peak may depend on the independent variables of detector type or the energy value of the peak because some detectors work better for different situations than others.

For the simulation the resolution is pre-defined as the standard deviation of the peak divided by the square root of the energy. In the first two simulations there are two peaks, 0.511 MeV and the 1.275 MeV energy values.

$$\frac{\sigma_{511}}{\sqrt{511\,\mathrm{keV}}} \approx \frac{\sigma_{1275}}{\sqrt{1275\,\mathrm{keV}}}$$

Simulation of a Moving Ion

We are interested in simulating an ion moving at a relativistic speed and detecting the gamma radiation created by it. The detected radiation will be Doppler shifted relative to the radiation

produced in the rest frame of the ion (a gamma photon of 1 MeV). The equation for this shift is given by:

$$\omega' = \gamma\omega(1 - \beta cos(\theta))$$
$$tan(\theta') = \frac{sin(\theta)}{\gamma(cos(\theta) - \beta)}$$
$$\gamma = \frac{1}{\sqrt{1-\beta^2}}, \quad \beta = \frac{v}{c}$$

Where ω and ω' are the frequency in the ion frame and lab frame respectively, θ and θ' are the polar angles in each frame, and v is the relative velocity of the two frames. Specifically, θ' is measured as the angle between the center of the detector face and the moving ion in the rest frame of the detector (lab frame).

Results

Correlation

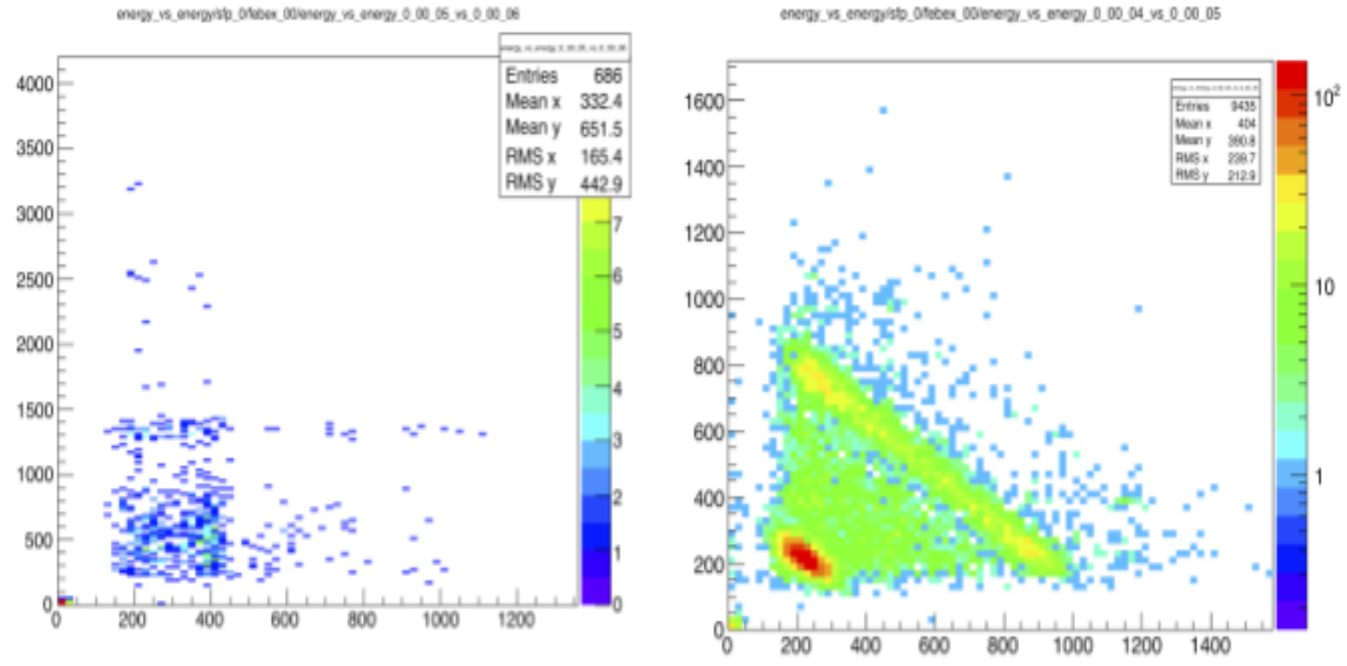

Fig 2: On the left is the correlation between one of the crystals in the large detector and the crystal in the small detector in the experiment. On the right is the correlation of the two crystals in the large detector in the experiment

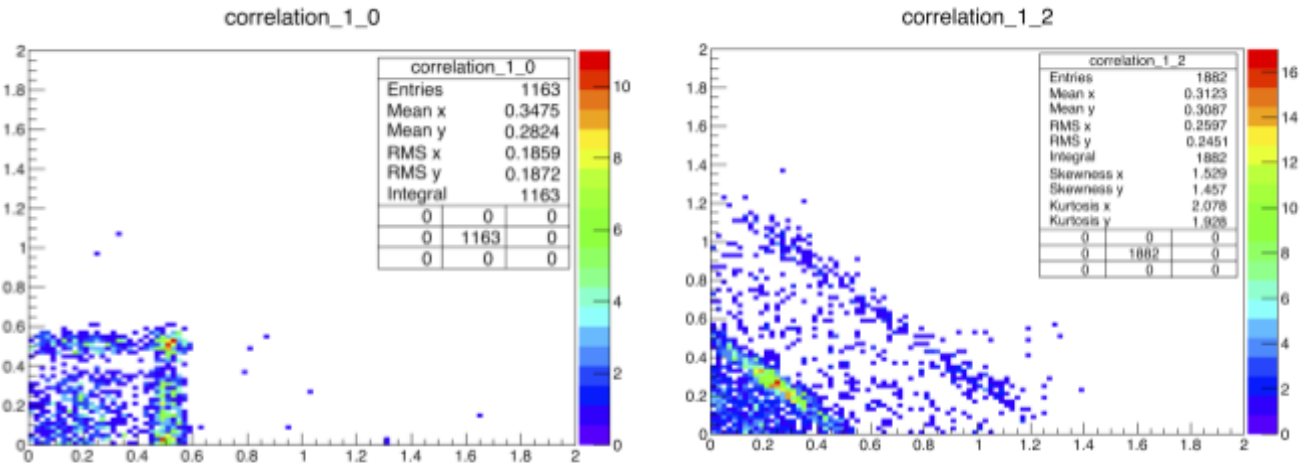

Fig 3: On the left is the correlation between one of the crystals in the large detector and the crystal in the small detector in the simulation. On the right is the correlation of the two crystals in the large detector in the simulation

Efficiency of the Detector

The efficiency of the detector was estimated from the ratio of the total efficiency and the geometric efficiency for both the higher energy peak at 1.275 MeV and the lower energy peak 0.511 MeV. The total efficiency in the experiment depends on the number of events registered by the detector for each photo-peak divided by the total product of the activity of the source, the fraction of the photons generated (per decay and energy) and the runtime. Where the fractions for gamma decay is 1.807 per decay for 0.511 MeV and 0.9994 per decay for 1.275 MeV. The current activity of Na is estimated from the last measured activity (A_0) and then multiplied by the runtime of the experiment, 779 s, and the two fractions for the different energies. Where the activity is:

$$A(t = 4.5\ yrs) = A_0 exp(-(t \cdot ln2)/t_{1/2})\ \text{[Bq]}$$

Where A_0 is the activity at t=0s , (Nov. 1st 2013) units of Becquerel [Bq], and $t_{1/2}$ is the half life of sodium (2.6 yrs).

$$Efficiency_{\ tot} = \frac{constant}{A(t)*\gamma*runtime}$$

where the ‘constant’ variable in the numerator is the integrated value of the number of events in the Gaussian fit.

Table 1: The small detector efficiency evaluated from the total efficiency against the geometric efficiency for the Gaussian fitted energy peaks. The 'without' case is a simulation performed without the large detector and the 'with' case is the simulation with the large detector placed on the opposite side of the source at an equal distance as the small crystal. In the simulation without the large detector the source-detector distance was 3.50 cm and in the case with the large detector, both the detectors were placed at an distance of 4.95 cm from the source as in the experimental set-up.

Small Crystal	**0.511 keV**	**1.275 keV**
ε_{det} **(without)**	1.42e-02	6.49e-04
ε_{det} **(with)**	2.26e-03	5.78e-04

The total efficiency results of the small crystal in the first simulation without the large detector and with the large detector in simulation 2 yields:

Simulation **without** the large detector: $\varepsilon_{tot} = 0.0126$

Simulation **with** large detector: $\varepsilon_{tot} = 0.0051$

which were calculated from the total number of registered events (of all energies) over the number of simulated number of events (1 milion).

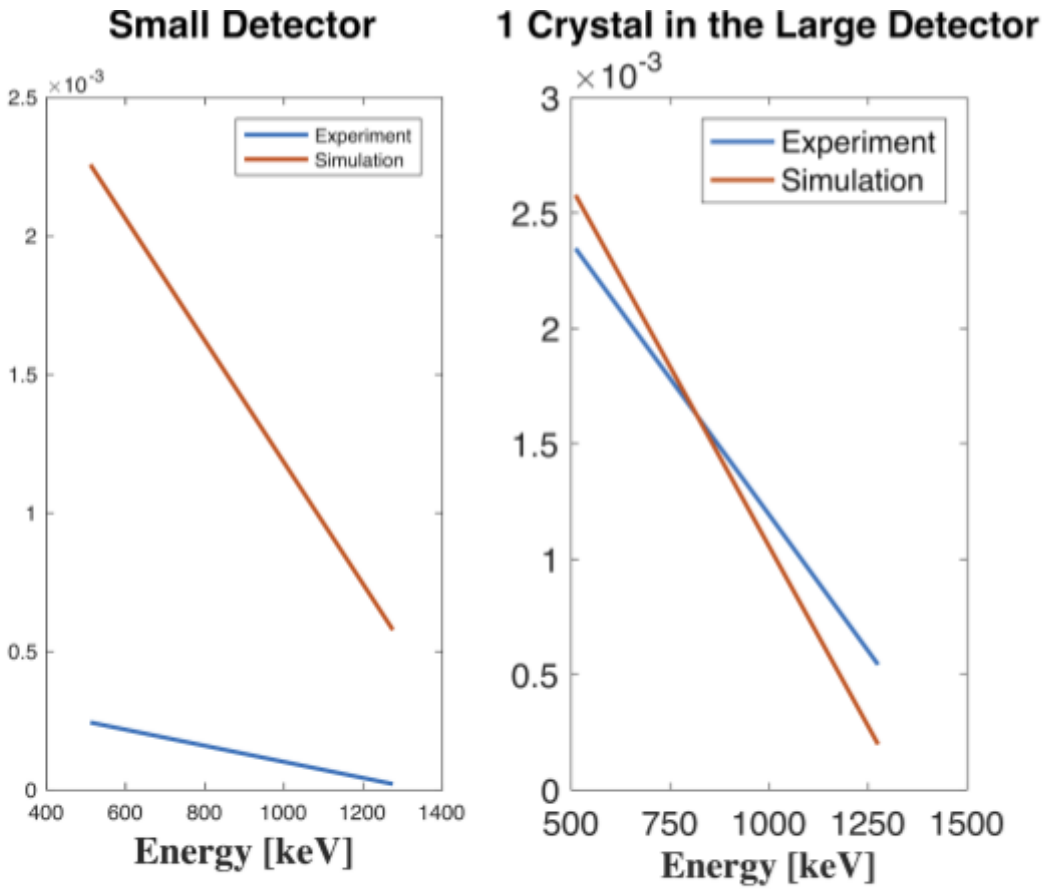

Fig. 4: Comparison between the detector efficiency of the experiment and the simulation for the small crystal and one of the crystals in the large detector.

Resolution

For the experiment the resolution is estimated from the FWHM and mean of the Gaussian fitted peaks. The simulation was also performed for a Germanium (Ge) semiconductor, see fig.6 crystal. No Gaussian fits were performed however, this was plotted for comparison with the CsI detector.

Table 2: The calculated relative resolution for the experiment from the ratio of the FWHM and the mean of the Gaussian fitted peaks.

	0.511 MeV	1.275 MeV
Large I	14 %	6.9 %
Large II	15 %	8.3 %
Small	7.9 %	5.5 %

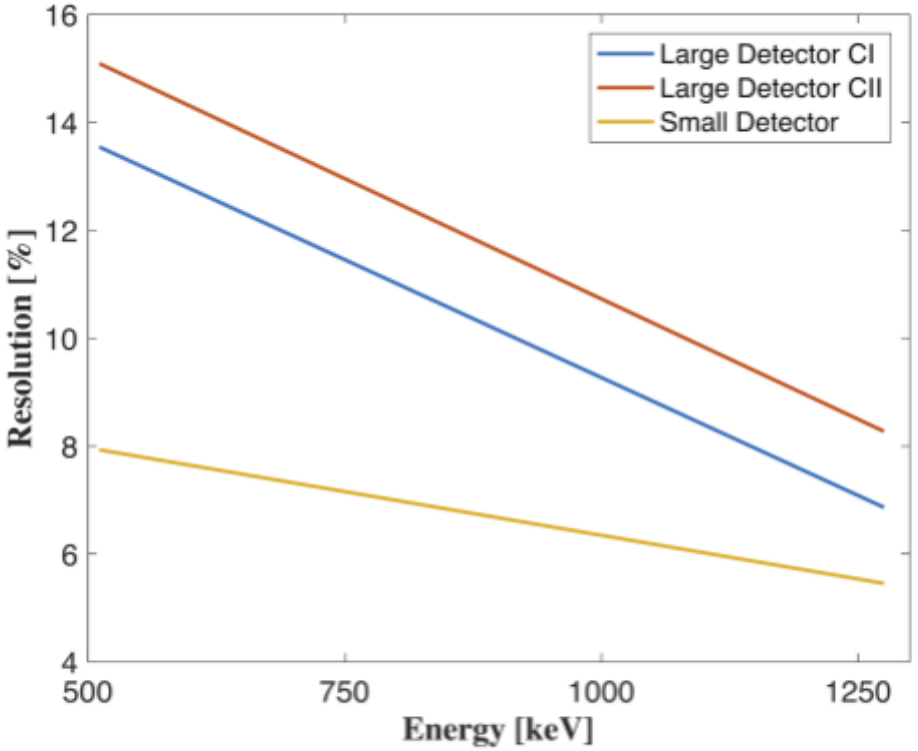

Fig. 5: The relative energy resolution. Evaluated from the ratio of the FWHM and the mean for the gaussian fits of the energy peaks at 0.511 MeV and 1.275 MeV.

Comparison with the resolution requirement of the simulation for the different energy peaks after Gaussian fits:

Table 3: The resolution in the simulation is pre-set so that the width of the peak is proportional to the square-root of the peak energy. In order to evaluate if this also is true for the experiment, the standard deviations of the Gaussian fits are divided by the square-root of the peak energy. The resulting values should be approximately equal for the different energy peaks if the proportionality is true.

Proportionality	0.511 MeV	1.2 MeV
Crystal 1 Large Box	1.2	0.94
Crystal 2 Large Box	1.1	0.94
Small Crystal	0.94	2.1

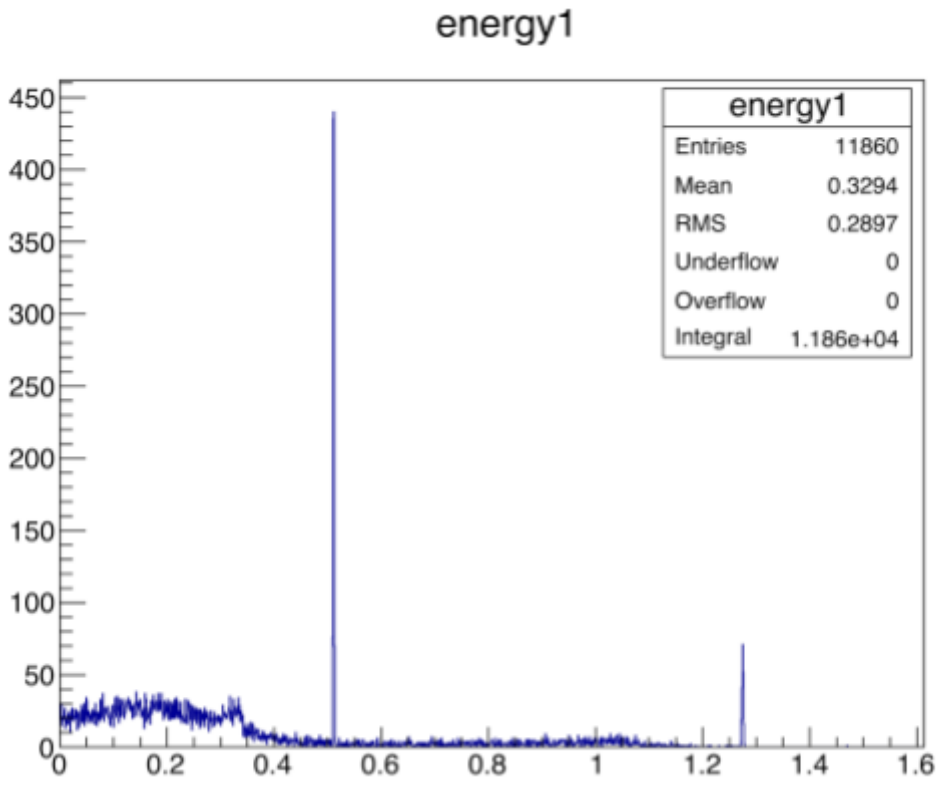

Fig. 6 : One of the histograms for the simulation with the Ge (semiconductor) detector. As indicated by the width of the peaks, the resolution is very high compared to a CsI crystal. These types of detectors are generally preferred for spectroscopy studies.

Movin Ion

With β = -0.7 and the energy of the moving energy was set to 1 MeV.

The energy in the moving frame of reference (ion-frame): $E_{mov} = E_{ion} * \gamma * \left(1 - \beta * cos\left(\theta_{fix}\right)\right)$

The energy in the fixed frame of reference (lab-frame): $E_{fix} = E_{ion} * \gamma * (1 - \beta * cos(\theta_{mov}))$

With the angle in the moving frame as $\theta_{mov} = arctan\left(\frac{sin(\theta)}{\gamma(cos(\theta) - (-\beta))}\right)$ and the θ_{fix} is given by the simulation for the different energy histograms.

Table 4: The result from the Gaussian fit of the simulation with moving ions and correction factor for the doppler shift for each angle and energy. The *E_theo* is the theoretically calculated energies from the random theta in the simulation.

CsI	sim4_E1 ~1.8	sim4_E5 ~0.7	sim4_E9~0.5
constant	408.9	381.3	132.2
mean	1.794	0.7163	0.4458
sig	0.1907	0.05943	0.03564
Entries	263757	82512	16773
theta [rad]	0.524	1.57	2.62
E_theo (moving)	2.2490 MeV	1.4011 MeV	0.55042 MeV
E_theo (fixed)	1.8129 MeV	0.71454 MeV	0.44442 MeV

Table 5 : The total efficiency of the spherical detector used for the moving ion simulation.

	Efficiency	Energy [MeV]
E1	4.1e-04	1.8
E5	3.8e-04	0.7
E9	1.3e-04	0.5

Discussion

Correlation

The plots to the left in fig. 2 and 3 display the correlation between the crystal in the small detector and one of the crystals in the large detector. This only represent the simultaneous detection of events in opposite direction occurring simultaneously.

Both the experiment and the simulation show two clear diagonal correlation lines, see the right plot in fig. 2 and 3. The experiment has around five times more events registered and therefore a higher intensity of correlation, however the experimental lines of correlation are located slightly more to the left and lower than the simulation. Clearly the simulation predicts correlations at the gamma energy peaks of 0.511 MeV and 1.275 MeV while the experiment yields slightly lower values, probably due to scattering in the detector (or in its casing) or before the detector.

The ‘addback’ method is in principle an integration, the sum of all the energies in the peak deposited in the crystal. Since just observing a discrete energy would yield too few events and due to scattering, the energy of the photons is not preserved but varies stochastically depending on which interactions took place before detection. For the correlation between the two crystals in the large detector, this is a representation of when both crystals detect an event more or less simultaneously. The event can be registered by both, if the photon is scattered from one detector to the other (if the detectors were side by side there would also be the possibility of the photon strikes the border of the detectors, however, here there is a spatial separation of 1 mm between the crystals). Since the detected photons have been scattered in one detector before reaching the other, they would have lost part of their energy before being completely absorbed by the other detector. The photons can also relinquish part of their energy in the second detector and consequently leave the detector without its initial energy being detected. In the event that the scattered gamma photon is absorbed in the second detector, then the sum of its registered events should represent the total energy of the incident gamma photon from the source. Therefor the sum of the axial values along the intensity diagonals equal the two energies 0.511 MeV (from beta decay) and 1.275 MeV from the gamma decay. The rest of the registered coincidences either represent cases where the photon has continued to scatter out of the detector without its total energy being detected. Alternatively, the photon could have been absorbed in a scattering processes such as the photoelectric effect, Compton scattering, pair-production, Auger electrons, Rayleigh scattering, Bragg scattering, neutron resonance scattering, or photo disintegration. All the scattering process have different probabilities depending on the energy of the incident photon and the atomic number of the absorber. There are not only several possible types of

scattering, one scattering process can also lead to another secondary or third process. Despite overestimating the total energy of coincidence, the simulation yields a good approximation in terms of the shape of the plot.

Efficiency of the Detector

Not surprisingly, the efficiency for the detectors are lower at higher energies. However, for the small detector, the result of the simulation deviates substantially from the actual experiment. In this case the experiment has a lot lower efficiency than expected from the simulation, see fig.4. The crystal thickness influences the probability of the photons interacting with the crystal, therefore the smallest crystal should in theory have lower efficiency because there is more likelihood that the photon passes through without being detected for the two different crystals of the same material.

The initial calculation of the detector efficiency deviated quite a lot for the small crystal in the first two simulations, with and without the larger detector, see table 1. This is probably due to the fact that different binning assignment was used for the Gaussian fits of the energy peaks. If instead, the total efficiencies are estimated from the complete number of detected entries versus the number of simulated events, then the efficiency for the small crystal in the simulation with and the simulation without the large detector differs by a factor of 2.6. Considering that in the first simulation the pre-set value for the source-to-detector distance was applied and in the second simulation this was altered to be the same distance as in the experimental set up, this is probably one of the causes of the decrease in efficiency since he distance has increased with 40 %.

Resolution

In fig. 5 and table 2, it is evident that the small crystal has a better resolution at the lower energy, however, for the higher energy peak there is not a great difference between the crystals. Since the crystals are all of the same material it is more likely that the difference is due to the dimension or placement of the crystals, both are placed in aluminum housings surrounded by an air gap. However the small crystal is much smaller in all dimensions and also significantly shorter in the longitudinal direction of detection from the source. The small crystal is 7 % (10 mm versus 130 mm) as long as the crystals in the large detector.

From Table 3, the proportionality of the resolution of the experiment can be indicated quite clearly for the large detector. The deviations in the case of the small detector could possibly be due to its different size, specifically since its thickness is much less, therefore less material for the photons to be absorbed into and the photons of higher energy are more likely to pass through without detection. In this case, the histogram also indicated a very low and broad peak as opposed to the narrow ones of the Ge detector in fig.6. Therefore, the resolution is much lower for the smaller detector than for the Ge detector.

In the case of the simulation with the Ge detector, the resolution is clearly (see fig. 6) much higher than with the CsI crystal. It is for this reason that semiconductor detectors are preferred in spectroscopy and radiation detection where one wants to avoid peak broadening. In this histogram we were unable to generate a Gaussian fit with ROOT.

Movin Ion

In the case of the simulation with moving ions, we changed the sign of β. The negative β allowed for beams to be simulated in all directions and not favour the forward direction (as with the positive β).

The theoretical estimation of the energy in the fixed (lab) frame, see table 4, coincides well with the energies from histograms in the simulation. The energies were calculated from the polar angle in the ion frame. ...

Only the total efficiency, table 5, was estimated since the geometric configuration is rather complex (for the extent of this exercise) and the solid angle for each element is rather small in the forward direction. Not surprisingly, the total efficiency is higher for the spherical detector, in particular for the higher energies. For the 0.511 MeV the total efficiency was estimated for simulation 2 to approximately $2.9*10^{-4}$, comparing to the moving ion simulation, the later is then 80 % more efficient. However, the detector in this case is more complex and more expensive to make.

Conclusion

The simulation worked quite well as an approximation. The results for the detector efficiency indicated that the experiment had a much lower efficiency than expected for the small crystal.

The conditions for the resolution in the simulation corresponds quite well with the experiment, except for at the high energy peak of 1.275 MeV for the small crystal.

For higher resolution, another type of detector is required, such as a semiconductor detector of highly purified germanium or a doped germanium semiconductor as can clearly be indicated by the histograms of the simulation with the Ge detector.

For the spherical detector in the moving ion simulations, the efficiency is higher for the higher energies as opposed to the cuboid detectors in simulation 2. However, the geometry is more complex and would require more time and money to actually construct.